Role of p53 in irinotecan-induced intestinal cell death and mucosal damage

Joanne M. Bowen[a,b], Rachel J. Gibson[a,b], Andrea M. Stringer[a,b], Thong W. Chan[c], Avanita S. Prabowo[c], Adrian G. Cummins[b,d] and Dorothy M.K. Keefe[a,b]

Irinotecan treatment of colorectal cancers results in high-grade intestinal mucositis in a large proportion of patients. The mechanisms behind irinotecan-induced mucosal injury, however, have yet to be fully explained. The aim of this study was to investigate the role of the p53 protein in the onset of intestinal damage following irinotecan treatment in two different settings. IEC-6 and FHs 74 intestinal cell lines were treated with irinotecan with and without a temporary p53 inhibitor, pifithrin-α, and examined for changes in proliferation and survival along with expression of p53 and related proteins. Forty tumour-bearing rats also underwent irinotecan treatment with and without pifithrin-α, and the effects on intestinal morphology, gene expression, apoptosis and other toxicities were assessed. Irinotecan caused a dose-dependent reduction in cell viability that was not prevented by pifithrin-α in either cell line. Rats responded to irinotecan with diarrhoea, weight loss, histopathological changes to the small and large intestine, increased crypt apoptosis, and a mild inflammatory response. Pifithrin-α reduced severity and duration of intestinal apoptosis; however, it did not significantly affect other parameters including p53 expression. Temporary inhibition of p53 activation does not markedly prevent intestinal cell death or mucositis following irinotecan treatment. Irinotecan may act through upregulation of proapoptotic proteins Bax and Bak to induce cell death. *Anti-Cancer Drugs* 18:197–210

Anti-Cancer Drugs 2007, **18**:197–210

Keywords: apoptosis, intestine, irinotecan, p53

[a]Department of Medical Oncology, Royal Adelaide Hospital, Departments of [b]Medicine and [c]Physiology, The University of Adelaide and [d]Department of Gastroenterology and Hepatology, The Queen Elizabeth Hospital, Adelaide, South Australia, Australia.

Correspondence to J.M. Bowen, Department of Medical Oncology, Royal Adelaide Hospital, North Terrace, Adelaide 5000, South Australia, Australia. Tel: +61 8 8222 3547; fax: +61 8 8222 3217; e-mail: joanne.bowen@adelaide.edu.au

Sponsorship: This work was carried out with support from a Royal Adelaide Hospital Internal Research Grant.

Received 16 May 2006 **Revised form accepted** 15 September 2006

Introduction

Cancer treatment-induced mucosal barrier injury, termed mucositis, is a common dose-limiting toxicity associated with chemotherapy [1]. Despite this, mucositis remains without a truly effective treatment or preventative solution. The hallmark histological features of intestinal mucositis include apoptosis, crypt hypoplasia, reduction in villous morphometry and increased permeability with or without inflammation [2,3]. At the patient level, symptoms include diarrhoea, abdominal pain, nausea, vomiting and ulceration [3,4]. It is yet to be completely elucidated as to which morphological and functional changes in the gut contribute to patient symptoms. It is, however, imperative that preventative therapies are designed in response to increased understanding of the pathogenesis of mucositis.

The topoisomerase I inhibitor, irinotecan (CPT-11), is a relatively new chemotherapy agent that is used commonly in the treatment of colorectal cancer [5–7]. Although effective against tumours, it also causes severe gastrointestinal mucositis (GIM) in a large proportion of patients, with the most frequent toxicity being severe diarrhoea [8,9]. The biochemical mechanisms for early- and late-onset diarrhoea induced by CPT-11 differ, and are thought to involve adverse cholinergic effects and direct mucosal damage, respectively [10–12]. Traditionally, investigations into the morphological effect of CPT-11 on the intestine have been conducted in rodent models receiving multiple doses of CPT-11 to induce mucositis [6,8,12–14]. From these studies, it is known that CPT-11 causes apoptosis early, which is followed by reductions in morphology.

Apoptosis is activated in response to DNA damage that can be controlled by the transcription factor, p53 [15–18]. The p53 protein regulates a number of downstream genes that act on the intrinsic and extrinsic apoptotic pathways. Targets along the intrinsic pathway include multiple members of the Bcl-2 family (Bax, Bak, Noxa, Puma, Bcl-2 and Bcl-x_L) [19–26]. It is believed that alterations in expression ratios of proapoptotic and antiapoptotic members of the Bcl-2 family control sensitivity of the cell to cytotoxic stimuli and ultimately its survival [27–31]. Another function of p53 is to activate genes required to arrest the cell cycle, i.e. $p21^{waf/cip-1}$ and 14-3-3 sigma

0959-4973

[32,33]. The p21 protein is a cyclin-dependent kinase inhibitor and once activated holds cells in G_1 phase [34]. It is thought that the combination of apoptosis and reduced proliferation contributes to loss of epithelial integrity in the intestine following cytotoxic therapy for cancer [3].

The requirement of p53 to transcriptionally activate genes to induce apoptosis and halt cell cycling can be exploited through blockade by chemical compounds [35,36]. The small compound, pifithrin-α (1-[4-methylphenyl]-2-[4,5,6,7-tetrahydro-2-imino-3(2H)-benzothiazoly]-ethane monohydrobromide), was identified as a temporary inhibitor of p53 that prevents movement of p53 into the nucleus following cytotoxic stimuli, hence rendering it unable to act as a transcription factor [37–39]. It has since been tested in various models of cancer treatment-induced cell death and shown to be effective at ameliorating damage [40–44].

The primary aim of this study was to examine the mechanisms controlling CPT-11-induced damage in the intestine using both in-vitro and in-vivo methods.

Methods

Cell lines

Both the IEC-6 (IEC) and FHs 74 (FHs) epithelial cell lines were obtained from the American Type Culture Collection (Manassas, Virginia, USA). IEC cells are derived from adult rat jejunum and display immunohistochemical markers characteristic of an undifferentiated crypt cell type. Assays using this cell line were carried out between passages 15 and 22. The FHs cells are derived from the small intestine of a human fetus and may contain some mesenchymal characteristics. Experiments were carried out on these cells between passages 24 and 30. Both cell lines retained their original morphology and growth characteristics over the range of passages used.

Cell culture

The IEC cell line was maintained in Dulbecco's modified Eagle's media supplemented to contain 1.5 g/l sodium bicarbonate, 4.5 g/l glucose, 50 U/ml penicillin, 50 μg/ml gentamycin, 1 μg/ml fungizome, 4 mmol/l L-glutamine, 10 μg/ml bovine insulin and 10% fetal calf serum (FCS). The FHs cell line was maintained in Dulbecco's modified Eagle's media supplemented to contain 1.5 g/l sodium bicarbonate, 4.5 g/l glucose, 50 U/ml penicillin, 50 μg/ml gentamycin, 1 μg/ml fungizome, 2 mmol/l L-glutamine, 0.9 × nonessential aminoacid solution, 0.9 mmol/l sodium pyruvate, 1 mmol/l oxaloacetic acid, 10 μg/ml recombinant human insulin, 30 ng/ml epidermal growth factor and 10% fetal calf serum (Gibco/BRL, Breda Netherlands). Cells were kept in sterile plastic culture flasks in a humidified atmosphere of 95% air with 5% CO_2 at 37°C.

Cell lines were routinely passaged using trypsin when culture monolayers reached approximately 80% confluence. Cells were subcultured at ratios between 1 : 3 and 1 : 6 in fresh growth medium. An assessment of cell number was carried out by addition of 0.4% trypan blue to an aliquot of cell suspension at a ratio of 1 : 1 and counted on a haemocytometer. Cell suspensions were diluted in fresh media to obtain a cell density of 1×10^5 cells/ml before reculturing.

Drug treatment

CPT-11 was a generous donation from Pfizer (Kalamazoo, Michigan, USA) and was kept at a concentration of 20 mg/ml diluted in a sorbitol/lactic acid buffer as described previously [8]. Aqueous CPT-11 was stored at 4°C in a light-proof container under sterile conditions. All further dilutions of CPT-11 were in sorbitol/lactic acid buffer and carried out immediately before the experimental use.

Cell number assessment

To measure drug toxicity in epithelial cells, the methylene blue dye-binding assay was used to estimate adherent cell number. Cells were subcultured into 96-well plastic tissue culture plates at a density of 10 000 and 15 000 cells/well for IEC and FHs, respectively, in 200 μl of growth medium. After 36 h, CPT-11 was added to wells at differing concentrations with or without 10 μmol/l PFT for 24 h. At the end of the drug incubation period, cells were immediately washed twice with saline to remove all traces of medium. Cells were fixed with 100% methanol for 10 min before being covered with 10 mg/ml methylene blue (Sigma, Steinheim, Germany) in 0.01 mol/l sodium tetraborate (pH 8.5) for 30 min. Wells were washed with 0.01 mol/l sodium tetraborate (pH 8.5) to remove unbound dye. The bound dye was eluted by addition of 0.1 mol/l HCl/100% ETOH (1 : 1) to each well and quantified with an automated plate reader at wavelength 630 nm (Beckham Coulter, Miami, Florida, USA). The inhibitory concentration was calculated as

$$\text{Inhibitory concentration}\,(\%) = \frac{(1 - A_{630}\ \text{value treated})}{A_{630}\ \text{value control}} \times 100.$$

Cell proliferation assessment

To measure the proportion of cycling cells following drug treatment, the Cell Proliferation Kit II (XTT) (Roche, Basel, Switzerland) was used in multiwell reactions. Cells were subcultured into 96-well plastic tissue culture plates at the aforementioned cell densities in 200 μl of growth medium. After 36 h, CPT-11 was added to all wells at differing concentrations ± 10 μmol/l PFT for 24 h. At the end of the treatment period, the media was aspirated and replaced with 100 μl of fresh growth medium. Each well also received 50 μl of freshly prepared XTT labelling mixture (tetrazolium salt XTT and electron coupling reagent). Metabolically active cells cleave XTT to a soluble formazan dye that was quantitated after 6 h using

a scanning multiwell spectrophotometer at wavelength 490 nm. Inhibition of cell cycling was calculated as

$$\text{Cytostasis}\,(\%) = \frac{(A_{490}\ \text{value control} - A_{490}\ \text{value treated})}{A_{490}\ \text{value control}} \times 100.$$

Immunohistochemistry on intestinal cells

To visualize changes in protein expression patterns following cytotoxic treatment, cells were subcultured onto eight-chamber glass slides (TissueTek, Naperville, Illinois, USA) at a density of 4×10^4 cells/well in 400 µl of growth medium. Cells were treated with 20 µg/ml CPT-11 ± 10 µmol/l PFT for 24 h. Slide-attached cells were fixed in fresh 4% paraformaldehyde for 30 min at 4°C. Slides were then washed twice in phosphate-buffered saline (PBS) before being incubated with 3% H_2O_2 in PBS for 10 min. Slides were rinsed in PBS and underwent a blocking step with 20% goat serum in PBS for 20 min. Following this, the excess was removed and replaced with primary antibodies against Bax, Bak, Bcl-x_L and Mcl-1 (Santa Cruz Biotechnology, Santa Cruz, California, USA) diluted in PBS. Slides were incubated for 1 h at room temperature followed by three washes in PBS. Slides were incubated with a biotinylated secondary antibody (Ab), followed by ultra-streptavidin conjugated to horseradish peroxidase (HRP) (Signet Laboratories, Dedham, Massachusetts, USA) and finally diaminobenzidine chromogen in 0.03% hydrogen peroxide. Slides were counterstained in diluted Lillie–Mayer's haematoxylin, dehydrated and mounted.

Western blotting

To investigate overall protein expression, cells were grown to 80% confluence in 10-cm diameter sterile plastic tissue culture dishes. Cells were washed and given 10 ml of fresh media ± CPT-11 ± PFT and incubated for 24 h. Following the treatment, cells were washed twice with ice-cold sterile PBS and harvested into lysis buffer (10 mmol/l Tris, 150 mmol/l NaCl, 1 mmol/l ethylenediaminetetraacetic acid, 1% Triton X-100 + protease inhibitor cocktail; Roche). Following disruption of cell membranes, the cell suspensions were spun at 10 000 r.p.m. for 15 min at 4°C, and the supernate was collected, aliquoted and stored at −70°C.

Whole-cell lysates were prepared, normalized for total protein content and 20 µg of protein was fractionated by sodium dodecyl sulphate–polyacrylamide gel electrophoresis before being electroblotted onto nitrocellulose membranes. Membranes were blocked with 3% skim milk in Tris-buffered saline containing 0.1% Tween 20 for 2 h before immunoblotting. Membranes were probed with anti-p53 monoclonal (Novocastra, Newcastle upon Tyne, UK) and p21, Bax and Bak polyclonal Abs (Santa Cruz Biotechnology) overnight at 4°C. This was followed by rabbit anti-mouse and goat anti-rabbit IgG Ab's, respectively, conjugation to HRP (Dako, Glostrup, Denmark) and detection by enhanced chemiluminescence (Amersham Biosciences, Buckinghamshire, UK). Membranes were also probed with anti-β-actin monoclonal Ab (Sigma) followed by rabbit anti-mouse secondary conjugated to HRP (Dako) to control for actual protein concentration loaded. Visualized bands were evaluated by densitometry, using an Alpha Imager 2200 (Alpha Innotech, Sanleadro, California, USA).

Laboratory animals

This study was approved by the Animal Ethics Committees of the Institute of Medical and Veterinary Sciences, Adelaide and of the University of Adelaide, and complied with National Health and Research Council (Australia) Code of Practice for Animal Care in Research and Training (2004). Female Dark Agouti (DA) rats, aged 6–8 weeks and weighing approximately 160 g, were purchased from the Institute of Medical and Veterinary Sciences MedVet division, group housed and kept under a 12-h light/dark cycle with free access to food and water until the study commenced. All animals used in this study were tumour-bearing. The mammary adenocarcinoma has been used by our group for a number of years and its passage has been described elsewhere [45,46].

Experimental design

Forty female DA rats (weighing approximately 180 g) were implanted with a tumour inoculum of 4.0×10^6 cells in 0.2 ml of PBS subcutaneously into each flank and divided into eight groups as follows: (i) control day 0, (ii) CPT-11 day 0, (iii) CPT-11 + PFT day 0, (iv) PFT day 2, (v) control day 2, (vi) CPT-11 day 2, (vii) CPT-11 + PFT day 2 and (viii) PFT day 2. Tumours were allowed to grow for 9 days, after which rats in CPT-11-treated groups (2, 3, 6 and 7) were given a 200-mg/kg intraperitoneal injection on day designated 0 to induce mucositis. CPT-11 was administered in a sorbitol/lactic acid buffer (45 mg/ml sorbitol/0.9 mg/ml lactic acid) required for activation of the drug. Rats also received 0.01 mg/kg subcutaneous atropine immediately before CPT-11 to reduce cholinergic reaction to the treatment. The rats in groups receiving PFT (3, 4, 7 and 8) were administered the compound diluted in dimethylsulphoxide (2.2 mg/kg, intraperitoneal) immediately before CPT-11. Control group rats (1 and 5) received dimethylsulphoxide injection only. Daily body weight was recorded along with 4 × daily assessment of reaction to treatment. Animals were culled by CO_2 asphyxiation and cervical dislocation at 6 and 48 h (designated day 0 and day 2) after treatment. The gastrointestinal tract from the pyloric sphincter to the rectum was removed and flushed with sterile 0.9% w/v saline, and the weight of the small and large intestine recorded. Two centimeter samples of the jejunum at 25% of the length of the small intestine from the pylorus and from the mid-colon at 50% of the length of the large intestine were collected, and

fixed in 10% neutral-buffered formalin or in Clarke's fixative for further analysis.

Histological examination

Samples of the jejunum and colon were collected and formalin-fixed overnight for routine histological examination. Tissue was paraffin embedded before being sectioned at 4 μm, and routinely stained with haematoxylin and eosin. Slides were sent to specialist veterinary pathologist, Dr John Finnie, from the Institute of Medical and Veterinary Sciences, South Australia, for expert reporting.

Intestinal morphometry

Sections of the jejunum and colon were opened onto cardboard and fixed for 24 h in Clarke's fixative, before being transferred to 70% ethanol for storage. To investigate intestinal morphometry, tissues were firstly removed from cardboard, rehydrated gradually and hydrolysed in 1 mol/l HCl for 7 min at 60°C. Tissue was washed twice with double-distilled water and stained in Schiff's reagent. Tissue was microdissected using a cataract knife and stereomicroscope under × 20 magnification. Microdissected tissue was mounted in 45% (v/v) acetic acid to measure villous area and crypt lengths using a calibrated graticule. Villous area was calculated as a trapezoid approximation by measuring villous height, and apical and basal width. Villous area and crypt length correlate with villus and crypt epithelial cell populations, respectively [47]. The number of mitotic cells was also counted in 15 randomly selected whole crypts and recorded as a measure of proliferation.

Apoptosis measurement

Sections of the jejunum and colon were fixed in 10% neutral-buffered formalin for 24 h. Tissue was routinely processed through ethanol and xylene and embedded into paraffin wax. Sections of the intestine were cut at 4 μm and subjected to TdT-mediated dUTP nick end-labelling assay by the In Situ Cell Death Detection Kit AP (Roche) according to the manufacturer's instructions. The methodology used for labelling apoptotic cells was similar to that of Gavrieli *et al.* [48]. Slides were counterstained with Mayer's haematoxylin and mounted with glycerol aqueous medium. Apoptotic bodies were counted and recorded per crypt per 4-μm section in 150 crypts.

Immunohistochemical detection of proteins

Two consecutive 4-μm paraffin sections of the jejunum and colon were cut onto 3-aminopropyltriethoxy-silane-treated (Sigma) glass slides, dewaxed in xylene and rehydrated through graded alcohols to water. Of the two sections on each slide, one was designated as the negative control and the other as the experimental section. Slides were washed with PBS before heat-mediated antigen retrieval in 10 mmol/l citrate buffer (pH 6.0). Endogenous peroxidase activity was quenched with 3% hydrogen peroxide in methanol for 1 min, whereas nonspecific antigens were blocked with normal serum for 20 min. Elimination of endogenous avidin and biotin was carried out using a commercial avidin/biotin blocking kit (Vector Laboratories, Burlingame, California, USA) as per the manufacturer's instructions. Experimental sections were incubated overnight at 4°C with the primary Ab for Bcl-x_L, Bax, Bak, Bid, p21 (Santa Cruz Biotechnology) and p53, and proliferating cell nuclear antigen (PCNA) (Novocastra Laboratories) diluted in a solution of PBS with *2%* serum. Negative control sections had the primary Ab omitted and were incubated with the dilution buffer only. After stringent washes in PBS between each step, sections were incubated with a biotinylated secondary Ab , followed by ultra-streptavidin conjugated to HRP and finally diaminobenzidine chromogen in 0.03% hydrogen peroxide. Slides were counterstained in diluted Lillie–Mayer's haematoxylin, dehydrated and mounted. Each slide was evaluated blinded to treatment and scored according to the staining intensity as previously described [49].

Statistical analysis

Statistical analysis of culture experiments was carried out using the repeated-measures analysis of variance with the post-hoc test and Kruskal–Wallis test to identify differences between groups. Statistical analysis of results from the animal experiment was carried out using the one-way analysis of variance with Tukey's post-hoc test to identify differences between groups. *P* values less than 0.05 were considered statistically significant.

Results

Effect of chemotherapy on cell adherence

Methylene blue assays were carried out on both cell lines to determine the effect of CPT-11 on adherent cell number. First, 24-h CPT-11 treatment caused a dose-dependent decrease in IEC-6 cell number, reaching a plateau in cell loss for concentrations above 50 μg/ml. The FHs 74 cell line showed a similar response to CPT-11. A dose-dependent decrease was found in adherent cells that plateau at concentrations above 100 μg/ml. Doses below 5 μg/ml did not induce cell loss.

Effect of pifithrin-α on cell survival

The nature of cell death induced by CPT-11 was investigated by temporary suppression of the transcriptional activity of p53 to determine whether a p53-dependent pathway was being utilized. During methylene blue assays, addition of 10 μmol/l PFT immediately before 24-h cytotoxic drug incubation resulted in no significant improvement in cell number for either IEC-6 or FHs cell lines. To assess the proportion of cells that remain metabolically active following CPT-11 treatment, the XTT assay was employed. CPT-11 caused a dose-dependent decrease in cell cycling in each of the cell

lines. PFT did not provide statistically significant protection against cytostasis in either cell line (Fig. 1).

Effect of cytotoxic treatment on protein expression in intestinal cell lines

Proteins involved in p53-induced apoptosis were investigated following cytotoxic treatment in intestinal cell lines. Through Western blot analysis, it was found that the expression of p53 and its downstream target, p21, was not significantly increased in IEC or FHs cells by CPT-11 treatment at 24 h. Additional treatment with PFT also did not induce changes in expression of p53 or p21. Treatment with CPT-11 caused a marked increase in the proapoptotic proteins, Bax and Bak, in IEC cells. Treatment with CPT-11 did not cause a significant change in either Bax or Bak expression in FHs cells. Combining PFT with CPT-11 treatment did not alter changes in protein expression compared with treatment with CPT-11 alone (Fig. 2). Treatment of either cell line with PFT alone resulted in no change in protein expression compared with controls (data not shown).

Effect of cytotoxic treatment on Bcl-2 family expression in intestinal cells

IEC and FHs cells were grown on glass slides and subjected to immunohistochemistry to detect Bcl-2 family proteins. Treatment with CPT-11 caused a marked increase in the proapoptotic proteins, Bax and Bak, in IEC cells, with an increase from below 20% cells stained to above 80% of cells stained (Fig. 2). Treatment with

Fig. 1

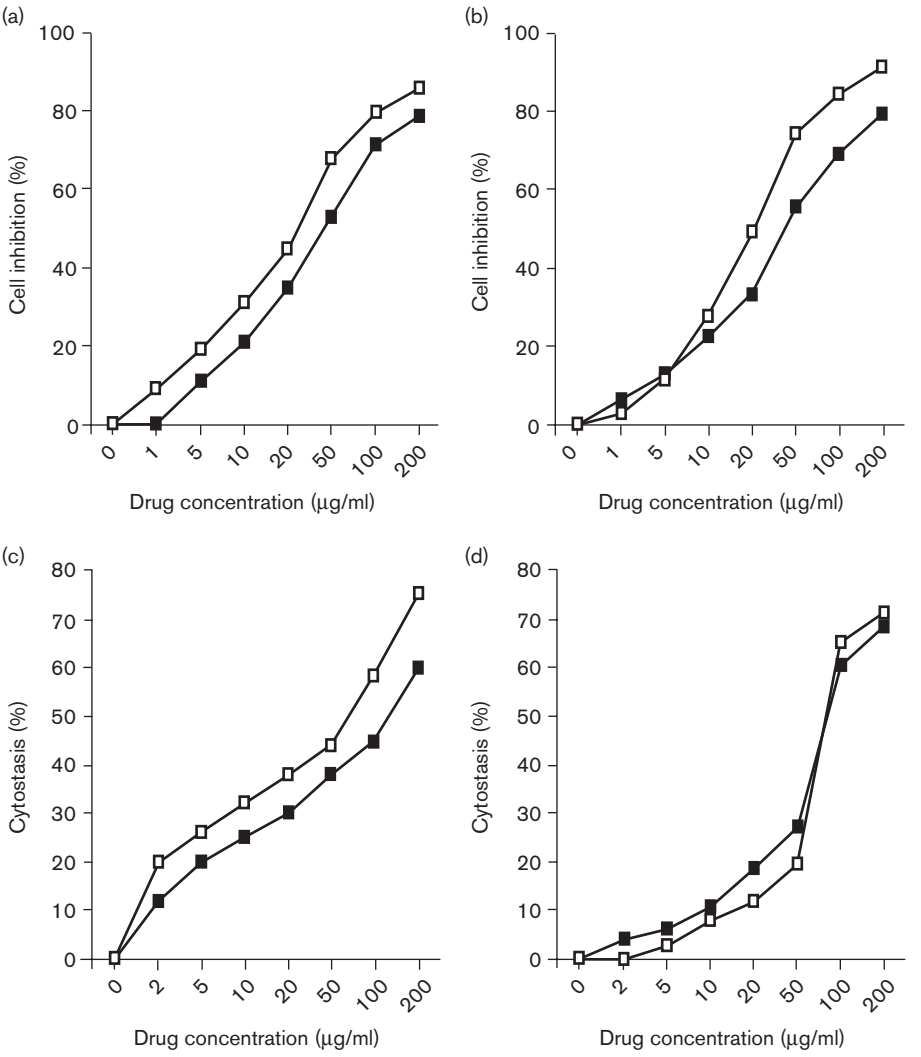

Effect of pifithrin-α (PFT) on adherent cell number and cellular proliferation following irinotecan (CPT-11) treatment in intestinal cells. Cell inhibition (a) IEC-6, (b) FHs 74, and cytostasis (c) IEC-6, (d) FHs 74 cell lines. Each experiment was repeated 3 times with four replications in each. Data presented is of group means. -□-, CPT-11; -■-, CPT-11 + PFT.

Fig. 2

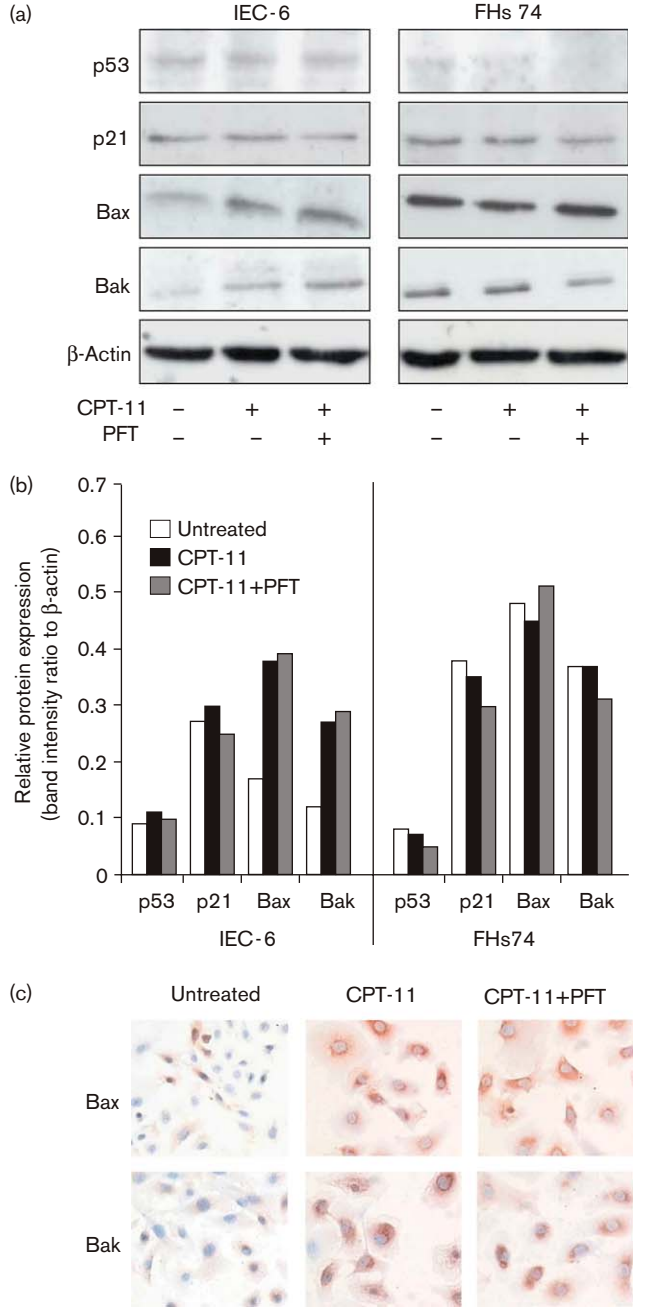

Effect of irinotecan (CPT-11) and pifithrin-α (PFT) treatment on protein expression in intestinal cells. Cells were incubated with 20 μg/ml CPT-11 for 24 h ± 10 μmol/l PFT. (a) Western blots show an increase in Bax and Bak expression in IEC-6 cells following irinotecan (CPT-11). (b) Graph of results for quantification of Western blot bands in both cell lines. (c) Photomicrographs of immunostaining for Bax and Bak in IEC-6 cells.

CPT-11 did not cause a significant change in either Bax or Bak expression in FHs cells. Weak cytoplasmic staining of Bcl-x_L was observed in approximately 50% of FHs cells that was unchanged by CPT-11. Less than 20% of IEC cells were positive for Bcl-x_L. They too had a very weak cytoplasmic staining, which was unaltered following treatment. Finally, Mcl-1 expression was reduced by CPT-11 in IEC cells, with a decrease from around 40% positively stained cells to below 10% following treatment; however, the expression was unchanged in FHs cells. Combining PFT with CPT-11 treatment did not alter changes in protein expression. Treatment of either cell line with PFT alone resulted in no change in the expression of Bcl-2 family proteins compared with controls.

Effect of irinotecan treatment on tumour-bearing rats

Treatment of rats with CPT-11 caused a number of adverse effects. CPT-11 caused mild diarrhoea in five out of six rats at 48 h. In the group that received PFT also, mild diarrhoea was seen in two rats. Atropine completely prevented early-onset diarrhoea. Rats in other groups showed no signs of diarrhoea at any time point. At 48 h, there was no significant difference in body weight for any group; however, rats treated with PFT + CPT-11 had regained some weight at this time point, whereas CPT-11-only rats continued to lose weight. Necropsy inspection found no significant difference in tumour weight between groups at 6 h or at 48 h. CPT-11 caused a significant reduction in small intestinal weight from 6 to 48 h in rats treated with PFT + CPT-11; however, large intestinal weight remained similar across groups at each time point.

Histopathological changes induced by irinotecan

Jejunum

Control rats showed no significant histological abnormality. CPT-11 treatment caused widespread apoptosis of enterocytes in basal regions of crypts at 6 h without other significant morphological changes. At 48 h, there was evidence of villous atrophy with clubbing of villi, loose eosinophil infiltration, lymphoplasmacytic infiltration of lamina propria and occasional individual apoptotic enterocytes. Regenerative hyperplasia was also present at this time point. The addition of PFT resulted in increased enterocyte hyperplasia and inflammatory infiltrate (Fig. 3).

Colon

No significant histological changes were observed in rats that were not treated with CPT-11. Sections that received CPT-11 showed widely distributed apoptosis of individual or small groups of crypt enterocytes and scant inflammation at 6 h. At 48 h, there was patchy to numerous dilated crypts, lined by attenuated epithelium. Occasional desquamated necrotic enterocytes were visible in the lumen and there was scant inflammation. No distinguishable differences were found between rats treated with PFT + CPT-11 or chemotherapy only (Fig. 4).

Fig. 3

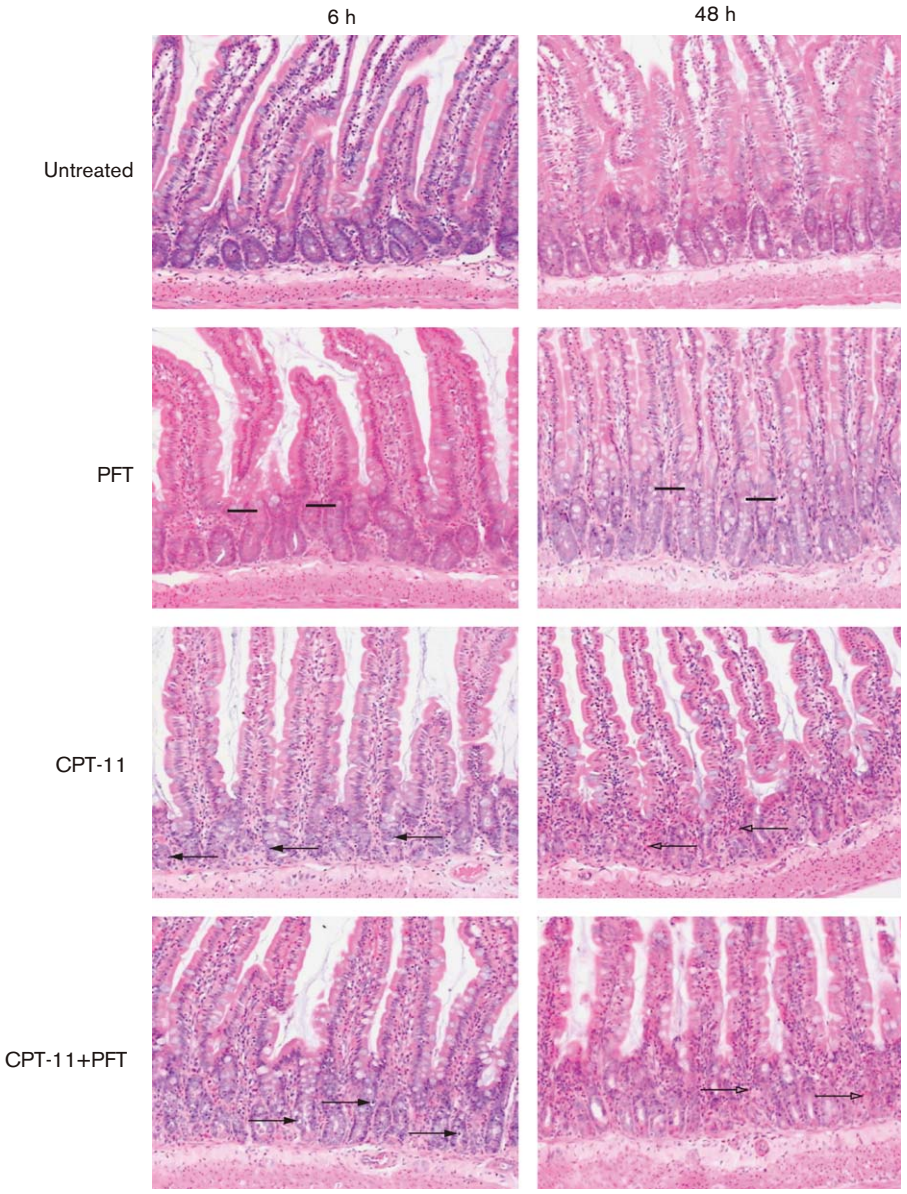

Photomicrographs of haematoxylin and eosin-stained rat jejunum. At 6 h following irinotecan (CPT-11), apoptotic cells were present within damaged crypts, as indicated by arrows with closed heads. By 48 h, there was evidence of inflammation, with loose eosinophil infiltrate, indicated by arrows with open heads. Pifithrin-α (PFT) caused crypt hyperplasia, as indicated with bars. Original magnification × 100.

Morphological changes induced by irinotecan

Jejunum

Rats treated with CPT-11 had a significant reduction in crypt length at 48 h ($P < 0.001$), which was not ameliorated by PFT ($P < 0.001$). All other groups had similar crypt lengths. Rats treated with CPT-11 had a significant reduction in villous area at 48 h ($P < 0.05$). PFT did not protect from CPT-11-induced reductions in villous area ($P < 0.05$). All other groups were not statistically different. CPT-11 caused a significant reduction in proliferation within jejunal crypts at 6 h ($P < 0.001$) and 48 h ($P < 0.001$) compared with controls. A trend occurred towards improvement in cell cycling by 48 h; however, this was not considered statistically significant. Combined treatment with PFT resulted in identical results to CPT-11-only rats, with a peak decrease in proliferation at 6 h ($P < 0.001$), which remained significantly reduced at 48 h ($P < 0.001$). Control and PFT-only rats had similar levels of proliferation (Table 1).

Fig. 4

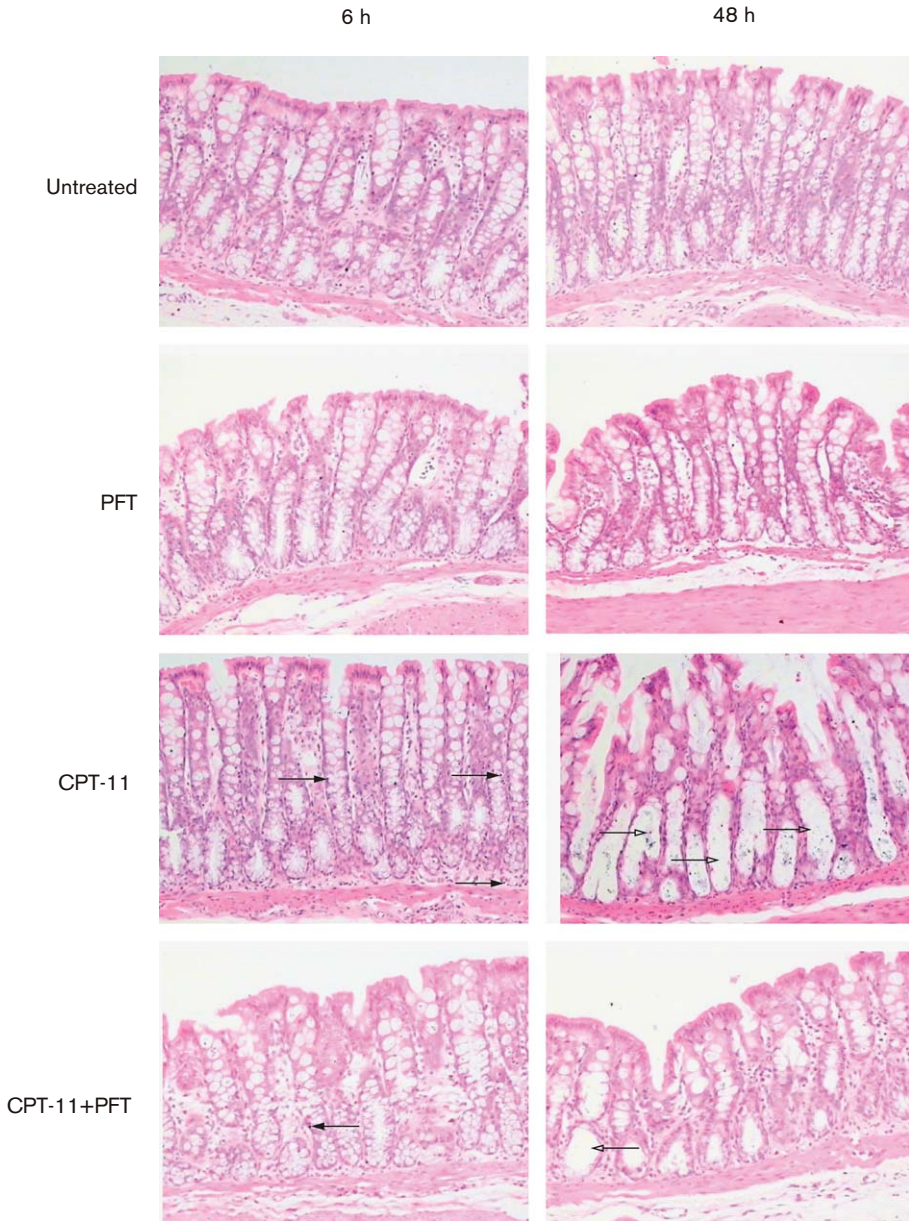

Photomicrographs of haematoxylin and eosin-stained rat colon. At 6 h following irinotecan (CPT-11), multiple apoptotic cells were present within damaged crypts, as indicated by arrows with closed heads. By 48 h, there were numerous dilated crypts with attenuated epithelium, indicated by arrows with open heads. Pifithrin-α (PFT) did not alter colonic histology. Original magnification × 100.

Colon

No significant differences were found in crypt length between groups at either time point. CPT-11 treatment resulted in a significant reduction in proliferation at 6 h only ($P < 0.05$). With the addition of PFT, proliferation was maintained in colonic crypts following CPT-11. Rats in PFT-only group had modestly increased proliferation at 48 h; however, this was not statistically more than in control rats (Table 1).

Apoptosis in intestinal crypts

Jejunum

A peak increase in apoptosis was seen at 6 h following CPT-11 ($P < 0.001$). Apoptosis was significantly reduced by 48 h ($P < 0.001$), but remained modestly higher than control levels ($P < 0.05$). Rats treated with CPT-11 + PFT also had a peak increase in apoptosis at 6 h ($P < 0.001$); however, by 48 h this had returned to control levels ($P < 0.001$). Rats in the control and

Table 1 **Effect of irinotecan (CPT-11) and pifithrin-α (PFT) treatment on apoptotic rate, proliferation and morphology in the rat intestine**

	Control		PFT		CPT-11		CPT + PFT	
	6 h	48 h	6 h	48 h	6 h	48 h	6 h	48 h
Apoptosis (jej)	0.12 ± 0.02	0.06 ± 0.02	0.06 ± 0.01	0.09 ± 0.01	5.77 ± 0.86#	0.97 ± 0.31*	4.55 ± 0.98#	0.61 ± 0.13
Apoptosis (col)	0.12 ± 0.01	0.07 ± 0.04	0.07 ± 0.02	0.04 ± 0.01	5.90 ± 0.59 ±	0.76 ± 0.21*	3.86 ± 0.54#+	0.31 ± 0.07
Mitosis (jej)	6.30 ± 0.66	5.93 ± 0.82	5.92 ± 0.41	6.16 ± 0.50	0.77 ± 0.33#	2.28 ± 0.46#	0.27 ± 0.11#	1.78 ± 0.48#
Mitosis (col)	2.10 ± 0.59	2.23 ± 0.32	2.15 ± 0.37	3.00 ± 0.49	0.42 ± 0.22*	1.85 ± 0.41	0.85 ± 0.40	2.30 ± 0.33
Crypt length (jej)	129.5 ± 5.42	135.5 ± 7.29	122.6 ± 4.78	135.4 ± 3.70	123.4 ± 2.00	94.4 ± 1.73#	124.5 ± 2.70	100.9 ± 3.37#
Crypt length (col)	288.3 ± 11.4	276.2 ± 7.70	267.2 ± 5.04	273.9 ± 9.45	270.9 ± 4.06	275.8 ± 7.89	278.3 ± 6.56	269.3 ± 9.26

Results shown are of group mean ± SEM ($n = 4–6$). Data for apoptosis, TUNEL-positive cells per crypt, for mitosis, proliferative cells identified by Schiff's staining per crypt; for crypt length, micrometers. Statistical significance compared with controls, where *; $P < 0.05$ and # $P < 0.001$. Statistical significance compared with CPT-11-only, where + $P < 0.001$.
PFT, pifithrin-α CPT-11, irinotecan, jej, jejunum, col, colon.

Fig. 5

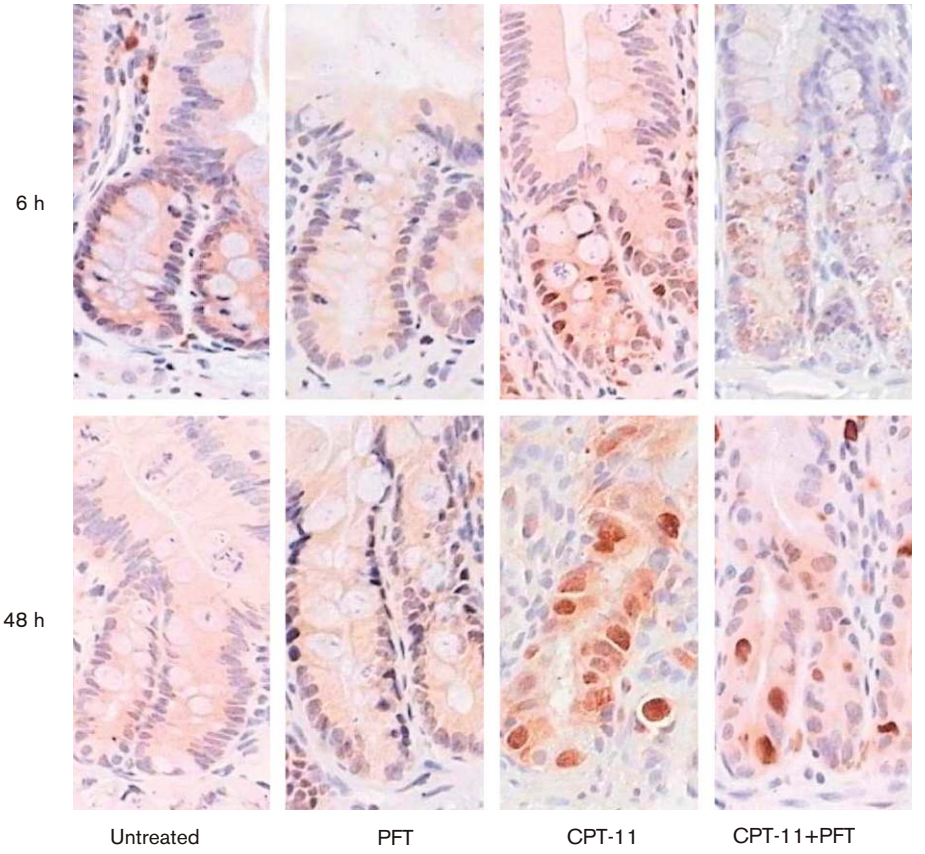

Photomicrographs of rat jejunum treated with irinotecan (CPT-11) and pifithrin-α (PFT). Immunohistochemical staining for p53 was increased modestly at 6 h and markedly at 48 h, which was partially ameliorated by PFT. Original magnification × 200.

PFT groups had similar low levels of apoptosis (Table 1).

Colon

CPT-11 caused a significant increase in apoptosis within colonic crypts that peaked at 6 h ($P < 0.001$) This reduced significantly by 48 h ($P < 0.001$), but remained slightly higher than control levels ($P < 0.05$). Treatment with CPT-11 + PFT also resulted in a peak increase in apoptosis at 6 h ($P < 0.001$), which was followed by a reduction to control levels at 48 h ($P < 0.001$); however, there was significantly more apoptosis in the crypts of rats treated with CPT-11 alone ($P < 0.01$) (Table 1).

Crypt protein expression following irinotecan *treatment p53*

In the jejunum, the tumour suppressor p53 protein could not be readily detected by immunohistochemistry in

Table 2 Quantification of immunostaining in rat intestinal crypts following cytotoxic treatment

	Control		PFT		CPT-11		CPT + PFT	
	6 h	48 h	6 h	48 h	6 h	48 h	6 h	48 h
Nuclear proteins (positive stained cells/crypt)								
p53 (jej)	0.05 ± 0.05	0.03 ± 0.07	0.27 ± 0.15	0.35 ± 0.11	3.22 ± 0.31*	5.13 ± 1.54#	0.78 ± 0.33+	2.02 ± 0.26*
p53 (col)	0.17 ± 0.08	0.13 ± 0.03	0.13 ± 0.06	0.13 ± 0.03	0.70 ± 0.17*	1.33 ± 1.29*	0.10 ± 0.05	0.85 ± 0.19*
p21 (jej)	0.15 ± 0.11	0.15 ± 0.04	0.10 ± 0	0.10 ± 0.07	0.90 ± 0.07	0.70 ± 0.09	0.20 ± 0	0.50 ± 0.14
p21 (col)	0.17 ± 0.03	0.2 ± 0	0.25 ± 0.04	0.27 ± 0.12	0.67 ± 0.08	0.43 ± 0.06	0.25 ± 0.04	0.57 ± 0.16
PCNA (jej)	16.2 ± 1.45	16.1 ± 1.04	18.2 ± 2.50	19.7 ± 1.25	8.9 ± 1.17#	8.49 ± 0.60#	11.3 ± 0.84*	10.5 ± 0.89*
PCNA (col)	14.6 ± 0.53	15.5 ± 1.26	11.3 ± 1.26	10.5 ± 2.08	11.62 ± 1.07	14.55 ± 0.37	17.3 ± 1.53	17.7 ± 1.63
Cytoplasmic proteins (staining intensity 0–4)								
Bax (jej)	1.67 ± 0.14	2.00 ± 0	1.75 ± 0.29	2.00 ± 0	2.83 ± 0.35	0.67 ± 0.18*	2.33 ± 0.14	0.75 ± 0.25*
Bax (col)								
ap	2.25 ± 0.18	2.25 ± 0.18	3.00 ± 0	1.75 ± 0.18	3.30 ± 0.29	2.67 ± 0.29	2.75 ± 0.18	2.68 ± 0.29
ba	1.25 ± 0.18	1.5 ± 0.29	2.00 ± 0	1.50 ± .035	2.67 ± 0.29	2.33 ± 0.29	2.50 ± 0.18	2.17 ± 0.38
Bak (jej)	2.25 ± 0.18	2.50 ± 0.25	2.25 ± 0.18	2.50 ± 0.35	2.33 ± 0.29	2.13 ± 0.38	2.33 ± 0.29	2.00 ± 0.25
Bak (col)								
ap	2.33 ± 0.29	2.17 ± 0.38	1.50 ± 0.10	1.50 ± 0.25	2.00 ± 0.50	1.33 ± 0.14	2.67 ± 0.14	1.00 ± 0.10
ba	1.50 ± 0.25	1.33 ± 0.14	1.67 ± 0.38	1.67 ± 0.14	2.67 ± 0.29*	1.67 ± 0.38	2.83 ± 0.14*	1.67 ± 0.38
Bid (jej)	2.00 ± 0	2.25 ± 0.18	2.00 ± 0.35	1.75 ± 0.18	1.25 ± 0.25	1.50 ± 0.25	0.75 ± 0.18	1.00 ± 0.25
Bid (col)								
ap	1.5 ± 0.35	1.5 ± 0.35	1.33 ± 0.14	1.5 ± 0.25	1.75 ± 0.18	1.75 ± 0.18	1.67 ± 0.29	1.67 ± 0.14
ba	0.75 ± 0.18	0.75 ± 0.18	0.67 ± 0.14	1.00 ± 0.25	1.00 ± 0.25	1.25 ± 0.18	1.00 ± 0.25	1.50 ± 0.25
Bcl-x_L (jej)	1.25 ± 0.18	1.5 ± 0.29	1.00 ± 0	1.25 ± 0.35	0.75 ± 0.18	0.50 ± 0	0.75 ± 0.18	0.50 ± 0.25
Bcl-x_L (col)								
ap	1.25 ± 0.18	1.00 ± 0.25	0.75 ± 0.18	1.33 ± 0.14	0.75 ± 0.18	0.33 ± 0.14	0.75 ± 0.14	0.67 ± 0.18
ba	0.5 ± 0	0.17 ± 0.14	0.50 ± 0	0.33 ± 0.14	0 ± 0	0.33 ± 0.14	0.50 ± 0	0.33 ± 0.14

Results shown are of group mean ± SEM (n = 4–6). Statistical significance compared with controls, where *P < 0.05 and #P < 0.001. Statistical significance compared with CPT-11-only, where +P < 0.001.
PFT, pifithrin-α; CPT-11, irinotecan; jej, jejunum; col, colon; ap, apical region of crypt; ba, basal region of crypt.

control or PFT-only treated rats at either time point. At 6 h, CPT-11 treatment caused a modest increase in p53 expression within the nuclei of jejunal crypt cells that was ameliorated by addition of PFT. At 48 h following CPT-11, there was a sustained increase in p53 expression with no significant differences in rat sections treated with PFT (Fig. 5). The expression of p53 in colonic crypts was sporadic in control sections and increased modestly following CPT-11 treatment. Treatment with CPT-11 + PFT at 6 h resulted in a slight decrease in overall p53 expression, whereas treatment with CPT-11 alone resulted in a concentration of cells expressing p53 in the mid crypt region. At 48 h following CPT-11, p53 expression was more evenly distributed through the lower half of crypts with or without PFT. Rats treated with PFT alone had similar expression levels of p53 within colonic crypts as other control rats at each time point (Table 2).

p21

The expression of $p21^{waf/cip-1}$ was not readily detectable in the crypts of the small and large intestine. Sections of the jejunum from rats in the control and PFT-only groups had very sporadic p21 staining, with less than one cell per five crypts being positive. At 6 h following CPT-11 treatment, p21 staining was increased slightly in sections not treated with PFT. The expression of p21 in sections at 48 h was similar in rats treated with CPT-11 with or without PFT. The degree of staining for p21 in the colonic crypts was also similar for each of the groups, in that it remained at an extremely low level (Table 2).

Proliferating cell nuclear antigen

Investigation of PCNA expression in the rat small intestine found that staining was present in all crypt cells located above crypt cell hierarchy position 1. Staining intensity and pattern was similar in control rats and those treated with PFT alone at both 6 and 48 h. CPT-11 treatment caused PCNA expression to contract to the stem cell region in the jejunum at 6 h. Addition of PFT partially maintained PCNA expression, with positive staining of cells present along most of the crypt length. At 48 h following CPT-11, PCNA positively stained cells were present along the entire remaining crypt length; however, the intensity of expression was markedly reduced compared with control sections. Furthermore, the crypts were considerably shorter, contributing to the reduction in number of PCNA-stained cells at this time point. Within the colon, PCNA was expressed in each cell in the lower two-thirds of every crypt within control and PFT-only sections. At 6 h following CPT-11, staining was reduced and was present in cells in the lower half of the crypt only, which was not prevented by PFT. Apoptotic cells expressed PCNA strongly. The expression of PCNA had increased, although not to control levels, by 48 h following treatment in the CPT-11-only group. The expression of PCNA was completely restored in CPT-11 + PFT-treated rats by 48 h. Treatment with PFT alone

Fig. 6

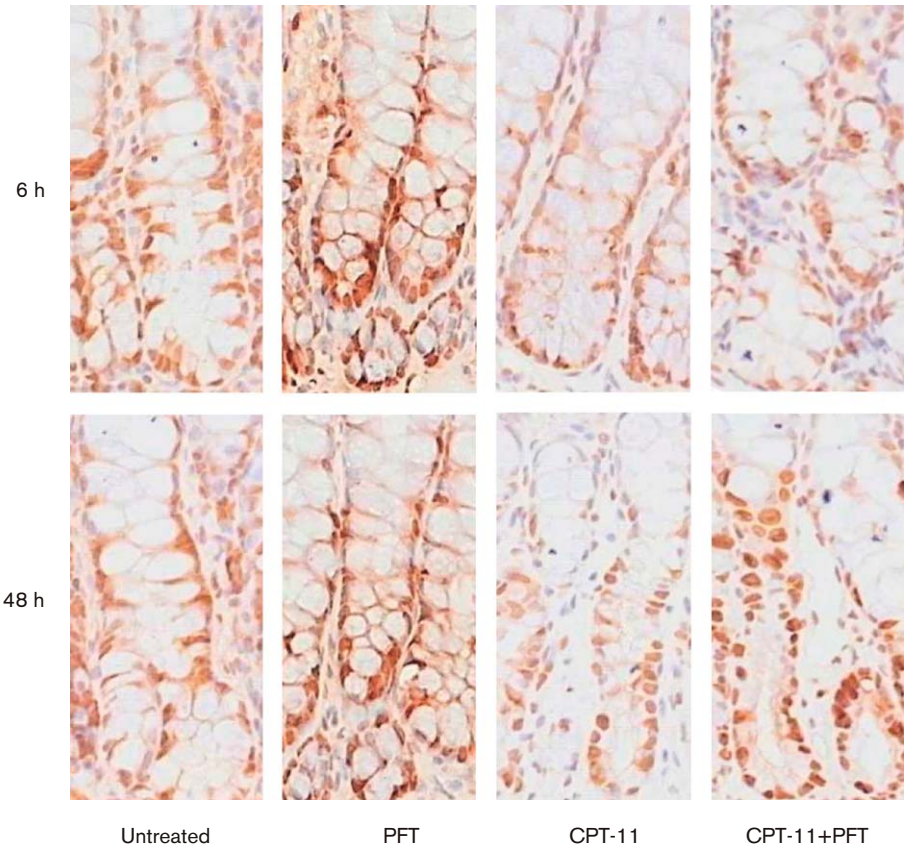

Photomicrographs of rat colon treated with irinotecan (CPT-11) and pifithrin-α (PFT). Immunohistochemical staining for proliferating cell nuclear antigen was decreased markedly at 6 h and returned to untreated levels by 48 h in rats treated with PFT. Original magnification ×200.

caused a modest increase in PCNA staining within the intestine (Table 2) (Fig. 6).

Bax

Sections from control rats and those treated with PFT alone had weak to moderate proapoptotic Bax staining in the cytoplasm of crypt cells and very weak staining of villous enterocytes. Cells undergoing late-stage apoptosis exhibited strong Bax staining. PFT slightly reduced Bax expression within apoptotic enterocytes in jejunal crypts, but did not reduce overall expression levels following CPT-11. At 48 h following CPT-11, Bax expression was significantly reduced in both treatment groups. Bax staining in the colon was strong in the luminal half of the crypt and weaker in the basal half of the crypt. Treatment with CPT-11 did not cause a significant increase in staining (Table 2).

Bak

Within the jejunum, control and PFT-only rats had strong cytoplasmic staining of both crypt and villous enterocytes. Furthermore, there was no measurable change in staining intensity for any treatment at either time point. Conversely, Bak expression was significantly increased at 6 h in the crypts of the colon in both CPT-11-treated groups. Staining intensity had returned to control levels by 48 h for CPT-11-only and CPT-11 + PFT groups. Treatment with PFT alone caused no observable change in proapoptotic Bak expression (Table 2).

Bid

The full-length proapoptotic Bid protein was detected in the nuclei and cytoplasm of control rat enterocytes. Almost all cells within jejunal crypts were moderately stained, which was then reduced following CPT-11 treatment. This was especially evident at 48 h, where remaining staining localized to nucleoli. Expression of Bid was weaker in the colon than in the jejunum. A gradient of expression from weak to moderate from the base of the crypt to the apical region was noticeable in control sections. This gradient was not evident in treated sections. No measurable difference was found in colonic crypt staining between groups (Table 2).

Bcl-x_L

Jejunal crypt cells had weak cytoplasmic staining that was decreased to extremely weak levels at 6 h by CPT-11 treatment. Antiapoptotic Bcl-x_L expression was not maintained by addition of PFT. Control and PFT-only treated rats had similar expression profiles at both time points. Within the colon, staining was weak along the length of the crypt until the apical table region where staining was absent. For this tissue region, no difference in the expression was noted at either time point for any group (Table 2).

Discussion

Cancer treatment agents damage the lining of the intestine and cause significant alterations in architecture and barrier function along with changes in gene expression. They are also known to induce apoptosis and restrict proliferation in epithelial crypts in the small and large intestine [2,50–53]. It has been postulated that these changes culminate in mucosal barrier injury. As such, the effect of CPT-11 on levels of apoptosis and cell cycling in intestinal epithelial cells was investigated, as was the nature of these cytotoxic effects through examination of associated changes in gene expression.

First, this study investigated multiple effects of CPT-11 treatment in normal intestinal cells and showed a dose-dependent decrease in cell viability, which is associated with increases in proapoptotic Bax and Bak protein expression. The effect on Bax and Bak, however, was limited to the rat intestinal cell line. This may be due to the inherent differences between the two species from which the cell lines were derived. To determine the role of p53 in chemotherapy-induced cell death in intestinal cells, a temporary p53 inhibitor, PFT, was included in a series of experiments. PFT was found to be ineffective at ameliorating cell inhibition and cytostasis following CPT-11 in both rat and human intestinal cell lines. This was confirmed by the lack of p53 expression in response to CPT-11 treatment in both intestinal cell lines, compared with strong p53 activation in the tumour-derived MCF-7 cell line (data not shown). It also did not have any effect on Bax or Bak expression. Thus the question remains, if apoptosis is occurring in a predominantly p53-independent fashion in response to chemotherapy treatment with CPT-11 in intestinal epithelial cells, then what is responsible for cell death in this setting? It is likely that generation of reactive oxygen species (ROS) in combination with direct DNA damage contributes to cellular injury. Activation of the transcription factor nuclear factor-κB (NF-κB) and its mediators by ROS has been implicated in the induction of mucositis [54,55]. Furthermore, a role for NF-κB is likely as PFT has no effect on its activation, unlike p53 [42] which may partly explain PFTs limited effects within this study. The proapoptotic role of NF-κB in mucosal toxicity in cancer patients is a field currently under intense investigation [56]. The possibility of intestinal cell lines carrying a p53 mutation was not investigated in this study, although this may explain the lack of activation following cytotoxic insult. The IEC-6 cell line, however, has previously been reported to have normal p53 [57,58], whereas no reports exist for FHs 74.

Second, this study examined the effect of a single dose of CPT-11 on the intestine of the rat with breast cancer by concentrating on mechanisms of p53-induced crypt damage. The approach was unique in that it investigated a combination of apoptotic, histological and morphological changes along with alterations in protein expression. CPT-11 caused deleterious effects in both the small and large bowel, which was partially ameliorated by temporary blockade of p53.

The DA rat breast carcinoma model was established to investigate GIM [8,12,45,46,59]. This study differed, however, from the traditional mucositis-inducing dosing protocol of two intraperitoneal injections to that of a single dose of 200 mg/kg CPT-11. The dual-dose administration of chemotherapy has previously been necessary, as a single dose of methotrexate caused an unreliable level of GIM, that was difficult to reproduce between experiments [60]. Administering multiple doses of chemotherapy on already damaged cells and tissues, however, made it difficult to assess changes in gene and protein expression, which are hypothesized to be critical in the development of GIM [61–63]. In this trial, single-dose CPT-11 treatment resulted in damage to both the small and large bowel, which was characterized by increased apoptosis within crypts and reductions in crypt cell cycling at 6 h. At 48 h, morphological alterations, especially villous clubbing and attenuation of crypt lining with or without regeneration, and slight inflammation were observed. These results correspond well with findings from previous multiple-dose studies [8,12] and confirm 200 mg/kg CPT-11 given intraperitoneally once is sufficient to cause GI changes that indicate early mucositis.

A primary aim of this study was to examine the effect of temporary inhibition of the transcriptional ability of p53 on the cytotoxicity of CPT-11. PFT was used to prevent movement of p53 into the nucleus of cells following insult, which resulted in a marginal improvement in the response to CPT-11. First, rats given PFT lost weight for less time that those treated with CPT-11 alone and the incidence of diarrhoea was reduced. It did not maintain morphology in the small or large intestine but limited the duration of apoptosis in the jejunum and colon, and also reduced the amount of apoptosis in colonic crypts. These results indicate that activation of the transcriptional function of p53 is not required for cell death in the

intestine, but instead acts synergistically with other CPT-11-induced genes. A possible explanation is that there is a direct interaction of cytoplasmic p53 with other inducers of cell death, i.e. Bax or Bak. Such a role for p53-induced activation of the caspase cascade without transcription has been reviewed previously [64].

To further characterize the role of CPT-11-induced damage in the intestine, a number of genes implicated as downstream effecters of p53-dependent apoptosis were examined [35]. This study found differential regulation of the proapoptotic Bcl-2 family proteins, Bax and Bak, in the jejunum and colon. The crypts of the jejunum upregulated Bax at 6 h following CPT-11 with strong expression in apoptotic cells. While, conversely, Bak was upregulated in colonic crypts treated with CPT-11 at 6 h. This is the first study to report a diversity in response of apoptotic proteins between the two intestinal regions following chemotherapy. It appears that Bax is the primary apoptosis regulator in the small intestine and Bak for the large intestine in response to CPT-11. It is worth noting also that the induction of Bax is not always strictly dependent on p53 [65] in so much as it does not require p53 transcriptional upregulation, which is blocked by PFT.

Immunohistochemistry confirmed the accumulation and change in subcellular location of the p53 protein following CPT-11. This, however, remained somewhat mild until 48 h, indicating that p53 was not responsible for the peak increase in apoptosis seen at 6 h. The p53-independent pathways to apoptosis that were activated could include ROS, ceramide and mitogen-activated protein kinase, all of which have been discussed extensively [66–69]. This finding complements the new biological explanation of alimentary mucositis proposed in recent reviews [61,70]. The concept of simultaneous damage occurring in multiple tissue layers, with activation of numerous cellular pathways, has implicated each of the aforementioned as well as others. It therefore seems likely that CPT-11 induces apoptosis and intestinal damage not via a p53-driven epithelial consequence but instead through a complex series of events involving several of the cell types in the GIT.

Acknowledgements

Ms Jaimi Burns and Ms Ann Yeoh are gratefully acknowledged for contributions made towards data collection and animal work.

References

1 Keefe DM, Gibson RJ, Hauer-Jensen M. Gastrointestinal mucositis. *Semin Oncol Nurs* 2004; **20**:38–47.
2 Keefe DM, Brealey J, Goland GJ, Cummins AG. Chemotherapy for cancer causes apoptosis that precedes hypoplasia in crypts of the small intestine in humans. *Gut* 2000; **47**:632–637.
3 Keefe DM. *The effect of cytotoxic chemotherapy on the mucosa of the small intestine [Thesis]*. Adelaide: University of Adelaide; 1998.
4 Pico J, Avila-Garavito A, Naccache P. Mucositis: its occurrence, consequences and treatment in the oncology setting. *Oncologist* 1998; **3**:446–451.
5 Ando Y, Hasegawa Y. Clinical pharmacogenetics of irinotecan (CPT-11). *Drug Metab Rev* 2005; **37**:565–574.
6 Ikuno N, Soda H, Watanabe M, Oka M. Irinotecan (CPT-11) and characteristic mucosal changes in the mouse ileum and cecum. *J Natl Cancer Inst* 1995; **87**:1876–1883.
7 Yu J, Shannon WD, Watson MA, McLeod HL. Gene expression profiling of the irinotecan pathway in colorectal cancer. *Clin Cancer Res* 2005; **11**:2053–2062.
8 Gibson RJ, Bowen JM, Inglis MR, Cummins AG, Keefe DM. Irinotecan causes severe small intestinal damage, as well as colonic damage, in the rat with implanted breast cancer. *J Gastroenterol Hepatol* 2003; **18**:1095–1100.
9 Abigerges D, Armand JP, Chabot GG, Da Costa L, Fadel E, Cote C, *et al.* Irinotecan (CPT-11) high-dose escalation using intensive high-dose loperamide to control diarrhea. *J Natl Cancer Inst* 1994; **86**:446–449.
10 Alimonti A, Gelibter A, Pavese I, Satta F, Cognetti F, Ferretti G, *et al.* New approaches to prevent intestinal toxicity of irinotecan-based regimens. *Cancer Treat Rev* 2004; **30**:555–562.
11 Yang X, Hu Z, Chan SY, Chan E, Goh BC, Duan W, *et al.* Novel agents that potentially inhibit irinotecan-induced diarrhea. *Curr Med Chem* 2005; **12**:1343–1358.
12 Gibson RJ, Bowen JM, Keefe DM. Palifermin reduces diarrhea and increases survival following irinotecan treatment in tumor-bearing DA rats. *Int J Cancer* 2005; **116**:464–470.
13 Cao S, Black JD, Troutt AB, Rustum YM. Interleukin 15 offers selective protection from irinotecan-induced intestinal toxicity in a preclinical animal model. *Cancer Res* 1998; **58**:3270–3274.
14 Trifan OC, Durham WF, Salazar VS, Horton J, Levine BD, Zweifel BS, *et al.* Cyclooxygenase-2 inhibition with celecoxib enhances antitumor efficacy and reduces diarrhea side effect of CPT-11. *Cancer Res* 2002; **62**:5778–5784.
15 Weller M. Predicting response to cancer chemotherapy: the role of p53. *Cell Tissue Res* 1998; **292**:435–445.
16 Merritt AJ, Potten CS, Kemp CJ, Hickman JA, Balmain A, Lane DP, *et al.* The role of p53 in spontaneous and radiation-induced apoptosis in the gastrointestinal tract of normal and p53-deficient mice. *Cancer Res* 1994; **54**:614–617.
17 Benchimol S. p53-dependent pathways of apoptosis. *Cell Death Differ* 2001; **8**:1049–1051.
18 Lowe SW, Ruley HE, Jacks T, Housman DE. p53-dependent apoptosis modulates the cytotoxicity of anticancer agents. *Cell* 1993; **74**:957–967.
19 Hershko T, Ginsberg D. Up-regulation of Bcl-2 homology 3 (BH3)-only proteins by E2F1 mediates apoptosis. *J Biol Chem* 2004; **279**:8627–8634.
20 Reinke V, Lozano G. Differential activation of p53 targets in cells treated with ultraviolet radiation that undergo both apoptosis and growth arrest. *Radiat Res* 1997; **148**:115–122.
21 Norbury CJ, Zhivotovsky B. DNA damage-induced apoptosis. *Oncogene* 2004; **23**:2797–2808.
22 Shibue T, Takeda K, Oda E, Tanaka H, Murasawa H, Takaoka A, *et al.* Integral role of Noxa in p53-mediated apoptotic response. *Genes Dev* 2003; **17**:2233–2238.
23 el-Deiry WS. Regulation of p53 downstream genes. *Semin Cancer Biol* 1998; **8**:345–357.
24 Sax JK, Fei P, Murphy ME, Bernhard E, Korsmeyer SJ, El-Deiry WS. BID regulation by p53 contributes to chemosensitivity. *Nat Cell Biol* 2002; **4**:842–849.
25 Muller M, Scaffidi CA, Galle PR, Stremmel W, Krammer PH. The role of p53 and the CD95 (APO-1/Fas) death system in chemotherapy-induced apoptosis. *Eur Cytokine Net* 1998; **9**:685–686.
26 Nita ME, Nagawa H, Tominaga O, Tsuno N, Fujii S, Sasaki S, *et al.* 5-Fluorouracil induces apoptosis in human colon cancer cell lines with modulation of Bcl-2 family proteins. *Br J Cancer* 1998; **78**:986–992.
27 Raisova M, Hossini AM, Eberle J, Riebeling C, Wieder T, Sturm I, *et al.* The Bax/Bcl-2 ratio determines the susceptibility of human melanoma cells to CD95/Fas-mediated apoptosis. *J Invest Dermatol* 2001; **117**:333–340.
28 Upadhyay S, Li G, Liu H, Chen YQ, Sarkar FH, Kim HR. bcl-2 suppresses expression of p21WAF1/CIP1 in breast epithelial cells. *Cancer Res* 1995; **55**:4520–4524.
29 Zong WX, Lindsten T, Ross AJ, MacGregor GR, Thompson CB. BH3-only proteins that bind pro-survival Bcl-2 family members fail to induce apoptosis in the absence of Bax and Bak. *Genes Dev* 2001; **15**:1481–1486.
30 Miyashita T, Krajewski S, Krajewska M, Wang HG, Lin HK, Liebermann DA, *et al.* Tumor suppressor p53 is a regulator of *bcl*-2 and *bax* gene expression *in vitro* and *in vivo*. *Oncogene* 1994; **9**:1799–1805.

31 Miyashita T, Reed JC. Tumor suppressor p53 is a direct transcriptional activator of the human *bax* gene. *Cell* 1995; **80**:293–299.
32 Vousden KH, Lu X. Live or let die: the cell's response to p53. *Nat Rev Cancer* 2002; **2**:594–604.
33 Fei P, Bernhard EJ, El-Deiry WS. Tissue-specific induction of p53 targets in vivo. *Cancer Res* 2002; **62**:7316–7327.
34 Harris SL, Levine AJ. The p53 pathway: positive and negative feedback loops. *Oncogene* 2005; **24**:2899–2908.
35 Kannan K, Amariglio N, Rechavi G, Jakob-Hirsch J, Kela I, Kaminski N, *et al.* DNA microarrays identification of primary and secondary target genes regulated by p53. *Oncogene* 2001; **20**:2225–2234.
36 Komarova EA, Gudkov AV. Chemoprotection from p53-dependent apoptosis: potential clinical applications of the p53 inhibitors. *Biochem Pharmacol* 2001; **62**:657–667.
37 Komarov PG. A chemical inhibitor of p53 that protects mice from the side effects of cancer therapy. *Science* 1999; **285**:1733–1737.
38 Gudkov AV, Komarova EA. Prospective therapeutic applications of p53 inhibitors. *Biochem Biophys Res Commun* 2005; **331**:726–736.
39 Gudkov A, Komarova E. Isolation of p53 inhibitors by screening chemical libraries in cell-based readout system. *Methods Mol Biol* 2003; **223**:635–648.
40 Zhang M, Liu W, Ding D, Salvi R. Pifithrin-α suppresses p53 and protects cochlear and vestibular hair cells from cisplatin-induced apoptosis. *Neuroscience* 2003; **120**:191–205.
41 Schafer T, Scheuer C, Roemer K, Menger MD, Vollmar B. Inhibition of p53 protects liver tissue against endotoxin-induced apoptotic and necrotic cell death. *FASEB J* 2003; **17**:660–667.
42 Komarova EA, Neznanov N, Komarov PG, Chernov MV, Wang K, Gudkov AV. p53 inhibitor pifithrin alpha can suppress heat shock and glucocorticoid signaling pathways. *J Biol Chem* 2003; **278**:15465–15468.
43 Culmsee C, Zhu X, Yu QS, Chan SL, Camandola S, Guo Z, *et al.* A synthetic inhibitor of p53 protects neurons against death induced by ischemic and excitotoxic insults, and amyloid beta-peptide. *J Neurochem* 2001; **77**:220–228.
44 Vollmar B, El-Gibaly AM, Scheuer C, Strik MW, Bruch HP, Menger MD. Acceleration of cutaneous wound healing by transient p53 inhibition. *Lab Invest* 2002; **82**:1063–1071.
45 Gibson RJ, Keefe DM, Clarke JM, Regester GO, Thompson FM, Goland GJ, *et al.* The effect of keratinocyte growth factor on tumour growth and small intestinal mucositis after chemotherapy in the rat with breast cancer. *Cancer Chemother Pharmacol* 2002; **50**:53–58.
46 Gibson RJ, Keefe DM, Thompson FM, Clarke JM, Goland GJ, Cummins AG. Effect of interleukin-11 on ameliorating intestinal damage after methotrexate treatment of breast cancer in rats. *Dig Dis Sci* 2002; **47**:2751–2757.
47 Cummins AG, LaBrooy JT, Stanley DP, Rowland R, Shearman DJ. Quantitative histological study of enteropathy associated with HIV infection. *Gut* 1990; **31**:317–321.
48 Gavrieli Y, Sherman Y, Ben-Sasson SA. Identification of programmed cell death *in situ* via specific labeling of nuclear DNA fragmentation. *J Cell Biol* 1992; **119**:493–501.
49 Bowen JM, Gibson RJ, Keefe DM, Cummins AG. Cytotoxic chemotherapy upregulate pro-apoptotic Bax and Bak in the small intestine of rats and humans. *Pathology* 2005; **37**:56–62.
50 Wilson JW, Pritchard DM, Hickman JA, Potten CS. Radiation-induced p53 and p21WAF-1/CIP1 expression in the murine intestinal epithelium: apoptosis and cell cycle arrest. *Am J Pathol* 1998; **153**:899–909.
51 Potten CS, Wilson JW, Booth C. Regulation and significance of apoptosis in the stem cells of the gastrointestinal epithelium. *Stem Cells* 1997; **15**:82–93.
52 Potten CS. Radiation, the ideal cytotoxic agent for studying the cell biology of tissues such as the small intestine. *Radiat Res* 2004; **161**:123–136.
53 Clavijo J, Gomez-de-Segura IA, Gomez-Garcia L, Vallejo-Cremades MT, Sanchez M, de Miguel E. Growth hormone protects the intestines but not the tumour from 5-fluorouracil toxicity in the short term in the rat. *Eur J Gastroenterol Hepatol* 2004; **16**:75–82.
54 Yeoh AS, Bowen JM, Gibson RJ, Keefe DM. Nuclear factor kappaB (NFkappaB) and cyclooxygenase-2 (Cox-2) expression in the irradiated colorectum is associated with subsequent histopathological changes. *Int J Radiat Oncol Biol Phys* 2005; **63**:1295–1303.
55 Van't Land B, Blijlevens NM, Marteijn J, Timal S, Donnelly JP, de Witte TJ, *et al.* Role of curcumin and the inhibition of NF-kappaB in the onset of chemotherapy-induced mucosal barrier injury. *Leukemia* 2004; **18**:276–284.
56 Sonis ST. The biologic role for nuclear factor-kappaB in disease and its potential involvement in mucosal injury associated with anti-neoplastic therapy. *Crit Rev Oral Biol Med* 2002; **13**:380–389.
57 Ray RM, McCormack SA, Johnson LR. Polyamine depletion arrests growth of IEC-6 and Caco-2 cells by different mechanisms. *Am J Physiol Gastrointest Liver Physiol* 2001; **281**:G37–G43.
58 Ray RM, Zimmerman BJ, McCormack SA, Patel TB, Johnson LR. Polyamine depletion arrests cell cycle and induces inhibitors $p21^{Waf1/Cip1}$, $p27^{Kip1}$, and p53 in IEC-6 cells. *Am J Physiol* 1999; **276 (3 Pt 1)**:C684–C691.
59 Gibson RJ, Bowen JM, Cummins AG, Keefe DM. Relationship between dose of methotrexate, apoptosis, p53/p21 expression and intestinal crypt proliferation in the rat. *Clin Exp Med* 2005; **4**:188–195.
60 Taminiau JA, Gall DG, Hamilton JR. Response of the rat small-intestine epithelium to methotrexate. *Gut* 1980; **21**:486–492.
61 Keefe DM. Gastrointestinal mucositis: a new biological model. *Support Care Cancer* 2004; **12**:6–9.
62 Sonis ST, Scherer J, Phelan S, Lucey CA, Barron JE, O'Donnell KE, *et al.* The gene expression sequence of radiated mucosa in an animal mucositis model. *Cell Proliferat* 2002; **35 (Suppl 1)**:93–102.
63 Sonis ST. A biological approach to mucositis. *J Support Oncol* 2004; **2**:21–32; discussion 35–36.
64 Moll UM, Zaika A. Nuclear and mitochondrial apoptotic pathways of p53. *FEBS Lett* 2001; **493**:65–69.
65 Bouvard V, Zaitchouk T, Vacher M, Duthu A, Canivet M, Choisy-Rossi C, *et al.* Tissue and cell-specific expression of the p53-target genes: *bax*, *fas*, *mdm2* and *waf1*/p21, before and following ionising irradiation in mice. *Oncogene* 2000; **19**:649–660.
66 Reed JC, Zhang J. Bcl-2 interrupts the ceramide-mediated pathway of cell death. *J Biol Chem* 1997; **272**:31482–31488.
67 Okuno S, Shimizu S, Ito T, Nomura M, Hamada E, Tsujimoto Y, *et al.* Bcl-2 prevents caspase-independent cell death. *J Biol Chem* 1998; **273**:34272–34277.
68 Kantrow SP, Gierman JL, Jaligam VR, Zhang P, Piantadosi CA, Summer WR, *et al.* Regulation of tumor necrosis factor cytotoxicity by calcineurin. *FEBS Lett* 2000; **483**:119–124.
69 Lamkanfi M, Kalai M, Saelens X, Declercq W, Vandenabeele P. Caspase-1 activates nuclear factor of the kappa-enhancer in B cells independently of its enzymatic activity. *J Biol Chem* 2004; **279**:24785–24793.
70 Sonis ST. The pathobiology of mucositis. *Nat Rev Cancer* 2004; **4**:277–284.